Article

Cancer Cell

Lactate Dehydrogenase B Controls Lysosome Activity and Autophagy in Cancer

Graphical Abstract

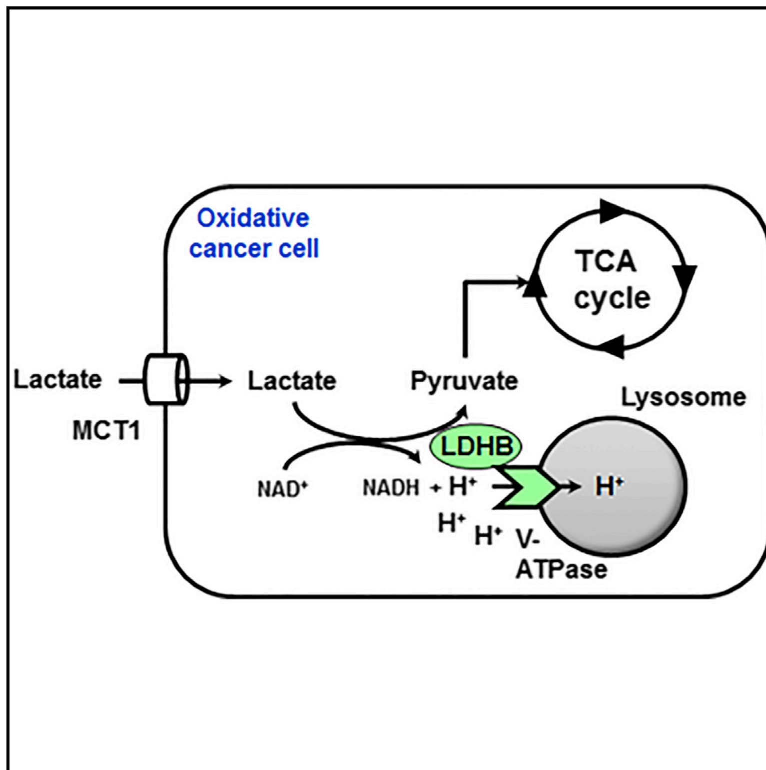

Authors

Lucie Brisson, Piotr Bański, Martina Sboarina, ..., Carine Michiels, Tamara Copetti, Pierre Sonveaux

Correspondence

pierre.sonveaux@uclouvain.be

In Brief

Brisson et al. show that lactate dehydrogenase B (LDHB) is critical for lysosomal activity and autophagy in cancer cells. Silencing LDHB selectively inhibits the proliferation of both oxidative and glycolytic cancer cells over normal cells, suggesting inhibition of LDHB as a promising anticancer approach.

Highlights

- Lactate supports lysosomal acidification and autophagy in cancer
- Lactate oxidation by LDHB yields protons that fuel lysosomal V-ATPase
- Targeting LDHB selectively blocks autophagy in oxidative and glycolytic cancer cells
- Targeting LDHB is a promising anticancer approach

Brisson et al., 2016, Cancer Cell *30*, 418–431
September 12, 2016 © 2016 Elsevier Inc.
http://dx.doi.org/10.1016/j.ccell.2016.08.005

CellPress

Lactate Dehydrogenase B Controls Lysosome Activity and Autophagy in Cancer

Lucie Brisson,[1] Piotr Bański,[1] Martina Sboarina,[1] Coralie Dethier,[1] Pierre Danhier,[1,2] Marie-Joséphine Fontenille,[1] Vincent F. Van Hée,[1] Thibaut Vazeille,[1] Morgane Tardy,[1] Jorge Falces,[1] Caroline Bouzin,[3] Paolo E. Porporato,[1] Raphaël Frédérick,[2] Carine Michiels,[4] Tamara Copetti,[1] and Pierre Sonveaux[1,5,*]

[1]Institut de Recherche Expérimentale et Clinique (IREC), Pole of Pharmacology, Université catholique de Louvain (UCL), 1200 Brussels, Belgium

[2]Louvain Drug Research Institute (LDRI), Université catholique de Louvain (UCL), 1200 Brussels, Belgium

[3]IREC Imaging Platform, Université catholique de Louvain (UCL), 1200 Brussels, Belgium

[4]URBC-NARILIS, University of Namur, 5000 Namur, Belgium

[5]Lead Contact

*Correspondence: pierre.sonveaux@uclouvain.be

http://dx.doi.org/10.1016/j.ccell.2016.08.005

SUMMARY

Metabolic adaptability is essential for tumor progression and includes cooperation between cancer cells with different metabolic phenotypes. Optimal glucose supply to glycolytic cancer cells occurs when oxidative cancer cells use lactate preferentially to glucose. However, using lactate instead of glucose mimics glucose deprivation, and glucose starvation induces autophagy. We report that lactate sustains autophagy in cancer. In cancer cells preferentially to normal cells, lactate dehydrogenase B (LDHB), catalyzing the conversion of lactate and NAD^+ to pyruvate, NADH and H^+, controls lysosomal acidification, vesicle maturation, and intracellular proteolysis. LDHB activity is necessary for basal autophagy and cancer cell proliferation not only in oxidative cancer cells but also in glycolytic cancer cells.

INTRODUCTION

Cancer can be viewed as a metabolic disease in which cancer cells strive to fulfill their proliferative agenda in a microenvironment characterized by uneven and fluctuating resource bioavailability. Oxygen and nutrient shortage are well-known characteristics of cancer that result from a mismatch between supply and use, inherent to blood perfusion abnormalities and high consumption rates (Walenta et al., 2001; Dewhirst et al., 2008). At least three different evolutionary metabolic strategies allow cancer cells to cope with fluctuating resource availability.

First, unlike most normal cells, cancer cells are characterized by a high metabolic plasticity allowing them to switch substrates depending on availability. While hypoxic cancer cells are addicted to glucose-fueled anaerobic glycolysis, oxidative cancer cells close to tumor-feeding blood vessels can use several precursor substrates in order to fuel oxidative phosphorylation, among which glucose, glutamine, lactate, and lipids represent the main available pools (Porporato et al., 2011; Dhup et al., 2012; Hensley et al., 2013). Fine-tuning the biosynthetic/bioenergetic balance is controlled at the enzymatic level to match cell needs (Warburg, 1956; Mazurek, 2011; Mullen et al., 2012).

Upon nutrient starvation, a metabolic strategy of cancer cells is to increase autophagy (White, 2012). During the autophagic process, an autophagosome is formed that isolates targeted or non-specific material. This content then undergoes enzymatic degradation after fusion of the autophagosome with lysosomes that provide protons and acid-activated proteases to the so-formed autolysosome (Levine and Kroemer, 2008). Degradation products can then be exported or recycled (Rabinowitz and White, 2010). Either excessive or long-term activation of autophagy or its inhibition with agents such as chloroquine may

Significance

Autophagy promotes cancer cell survival and proliferation by recycling damaged proteins and organelles in case of oxidative stress and by ensuring metabolite supplementation under nutrient starvation. We identified that lactate dehydrogenase B (LDHB) controls autophagy in cancer. LDHB catalyzes the conversion of lactate and NAD^+ to pyruvate, NADH, and H^+. This reaction promotes lysosomal acidification dependent on V-ATPase, a proton pump of lysosomes. Lysosomal acidification is essential for vesicle maturation and protease activation during autophagy. Consequently, lactate oxidation by LDHB promotes autophagy in oxidative and glycolytic cancer cells. Conversely, targeting LDHB activity inhibits autophagy and the proliferation of cancer cells preferentially to normal differentiated cells.

 © 2016 Elsevier Inc.

CrossMark

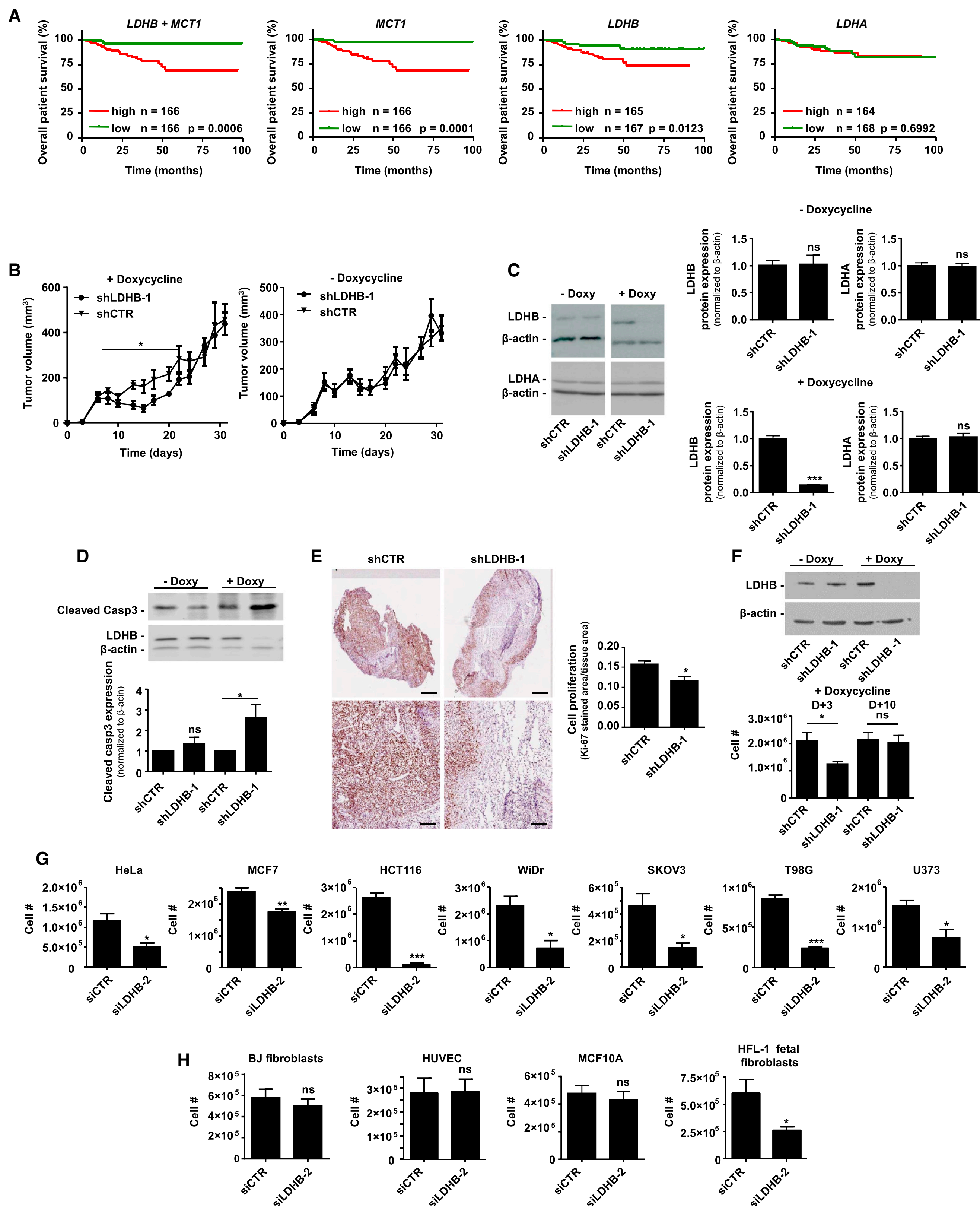

(legend on next page)

lead to cell death (Maclean et al., 2008; Yoon et al., 2010). Inhibition of autophagy in particular constitutes a promising therapeutic approach against cancer. Autophagy also offers cytoprotection by recycling damaged proteins and organelles when cancer cells face redox stress (White, 2012). Additional metabolic resources can be obtained when cancer cells exploit the metabolic activities of stromal cells, such as fibroblasts, adipocytes, and muscle cells (Commisso et al., 2013; Icard et al., 2014), an extreme form of which is cannibalism for nutrient and functional organelle supply (Krajcovic and Overholtzer, 2012; Tan et al., 2015).

A third metabolic strategy promoting tumor progression is cooperativeness. A good example is when oxidative cancer cells oxidatively recycle lactate provided by glycolytic cancer cells, thus sparing glucose and optimizing its bioavailability as a glycolytic fuel for hypoxic cancer cells (Sonveaux et al., 2008; Kennedy et al., 2013). The oxidative use of lactate by oxygenated cancer cells depends on its uptake, a process facilitated by monocarboxylate transporters (MCTs, of which MCT1 is the main contributor), and on the oxidation of lactate in pyruvate by lactate dehydrogenase B (LDHB). Pyruvate then fuels the tricarboxylic acid cycle (Dhup et al., 2012). This pathway represses glycolysis because of a competition between LDHB and the glycolytic enzyme glyceraldehyde-3-phosphate dehydrogenase for NAD^+ and owing to an allosteric inhibition of glycolytic enzymes hexokinase and phosphofructokinase-1 by lactate (Leite et al., 2011; Dhup et al., 2012). Cooperativeness based on the preferential use of lactate compared with glucose by oxidative cancer cells was coined metabolic symbiosis (Sonveaux et al., 2008). It is a hallmark of many cancer types (Sonveaux et al., 2008; Ho et al., 2012; Guillaumond et al., 2013; Curry et al., 2013; Kennedy et al., 2013). However, while improved glucose delivery is a net advantage for glycolytic cancer cells, its benefit for oxidative cancer cells is still elusive. This study addresses this open question.

RESULTS

LDHB Controls Tumor Progression and Cancer Cell Proliferation

Using oxidative SiHa human cervix adenocarcinoma cells as main model, we previously proposed that oxidative lactate metabolism is at the core of a metabolic symbiosis based on the exchange of lactate in cancer (Sonveaux et al., 2008; Dhup et al., 2012). This pathway requires MCT1-facilitated lactate uptake and lactate oxidation to pyruvate by LDHB (Halestrap and Wilson, 2012). To further demonstrate the significance of lactate oxidation in cancer, we retrospectively analyzed a microarray dataset of 332 uterine cancer patients. We found that high expression of *MCT1*/*SLC16A1* together with *LDHB* predicts poor overall patient survival (Figure 1A). Taken independently, *MCT1* and *LDHB* were significantly associated with poor patient prognosis, but *LDHA*, catalyzing the reduction of pyruvate to lactate in glycolytic cancer cells, was not. Clinical data thus suggested that, contrary to its closest relative LDHA, LDHB could control the clinical progression of uterine cancers. We therefore aimed to experimentally characterize the specific contribution of LDHB to tumor progression. We engineered SiHa cells expressing a TET-on small hairpin RNA (shRNA) targeting LDHB (shLDHB-1) or a control shRNA (shCTR), which were used to generate tumors in mice. To preserve tumor take, doxycycline was administered 1 day after tumor implantation. Compared with shCTR, doxycycline-induced shLDHB-1 expression caused significant yet transient tumor growth retardation (Figure 1B). Analysis of tumors at the end of the experiments revealed no re-expression of LDHB and no compensation of LDHB silencing by increased LDHA expression (Figure 1C). Silencing LDHB was associated with increased apoptosis (caspase-3 cleavage, Figure 1D) and decreased cell proliferation (Figure 1E). In vitro assays using the same system (cells were treated for 7 days with doxycycline, then an equal number of cells were plated for an additional 3 days of treatment with doxycycline) recapitulated our in vivo observations by showing an early but not a late decrease in SiHa cell number by shLDHB-1, despite effective LDHB silencing (Figure 1F). We used the same strategy to induce a second inducible shRNA (shLDHB-2) in mice bearing an HCT116 human colon carcinoma xenograft. Doxycycline was administered 12 days after tumor implantation once tumors reached 5 mm in diameter. Silencing LDHB caused significant HCT116 growth retardation (Figures S1A and S1B).

Our data indicated that, in cancers, LDHB controls early tumor progression and the number of cancer cells, and negatively affects patient survival. To better delineate the contribution of LDHB to malignancy, we tested other cancer cell lines. Silencing LDHB with a small interfering RNA (siRNA) (siLDHB-2) decreased cell number in all the cancer cell lines that we investigated: HeLa

Figure 1. Silencing LDHB Delays Tumor Growth and Decreases Cancer Cell Number

(A) SurvExpress gene expression database analysis of potential markers of overall survival in uterine cancer patients (n = 332 patients in total; 164–168 patients per group).

(B) Tumor growth of SiHa cancer cells carrying a TET-on control shRNA (shCTR) or a TET-on shRNA targeting LDHB (shLDHB-1) in mice treated with doxycycline (1 mg/mL) or vehicle via the drinking water starting 1 day after cell inoculation (n = 8 mice per group).

(C and D) LDHB and LDHA protein expression (C) and cleaved caspase-3 (D) in the lysates of tumors collected from animals killed at the end of the experiment (n = 8).

(E) Immunohistochemical detection and quantification of proliferation marker Ki-67 in tumors treated with doxycycline collected at the end of the experiment shown in (B) (scale bar represents 1 mm in the top panels and 200 μm in the bottom panels; n = 8).

(F) Representative western blots of SiHa cells harboring shCTR or shLDHB-1 treated with or without doxycycline (0.5 μg/mL) for 3 days and quantification of cell number after 3 and 10 days of treatment (n = 4). Results at day 10 involved replating an equal number of cells at day 7, then letting them grow for 3 more days.

(G) Cancer cells were transfected with a control siRNA (siCTR) or with siRNAs against LDHB (siLDHB-1 or siLDHB-2) and counted 72 hr later (n = 3–4).

(H) As in (G) but using nonmalignant cells (n = 4–6).

All data represent means ± SEM. *p < 0.05, **p < 0.001, ***p < 0.005; ns, not significant, by log rank test (A), two-way ANOVA (B), Mann-Whitney test (C and E), Wilcoxon matched-pairs signed rank test (D), one-way ANOVA and Holm-Sidak's multiple comparison test (F), or two-tailed unpaired Student's t test (G and H). See also Figure S1.

cervix cancer cells, MCF7 human breast cancer cells, HCT116 and WiDr human colon carcinoma cells, SKOV3 human ovarian carcinoma cells, and T98G and U373 human glioblastoma cells (Figures 1G, S1C, and S1D). Comparatively, siLDHB did not affect the number of normal differentiated BJ human skin fibroblasts, HUVECs (human umbilical vein endothelial cells), and MCF10A human mammary gland epithelial cells (Figures 1H and S1E). However, the number of fetal HLF-1 fibroblasts was decreased by siLDHB. These observations justified further molecular investigation.

Targeting LDHB Selectively Inhibits Basal Autophagic Flux in Oxidative Cancer Cells

In oxidative cancer cells, the oxidative use of lactate preferentially to glucose could mimic glucose deprivation (Sonveaux et al., 2008; Leite et al., 2011), and glucose deprivation stimulates autophagy. Because unlike normal cells most cancer cells have a high level of basal autophagy (White, 2012; Avalos et al., 2014), we hypothesized that LDHB could control autophagy in cancer. To test this hypothesis, we first investigated combinations of siLDHB with known inhibitors of autophagy: chloroquine (Maclean et al., 2008) and an siRNA targeting ULK1 (siULK1), a serine/threonine-protein kinase that activates autophagy by phosphorylating beclin-1 (Russell et al., 2013). Individually, siLDHB decreased SiHa cell number as efficiently as chloroquine (Figures 2A, S2A, and S2B) and siULK1 (Figure 2B). There was no additive effect when combining siLDHB with chloroquine or with siULK1, indicating that these inhibitors target the same biological pathway. siLDHB and siULK1 were also equally potent and had no additive effects when used in combination in HeLa oxidative cervix cancer cells (Figure S2C). We further verified in both cell lines that siLDHB did not influence ULK1 and that siULK1 did not influence LDHB protein expression (Figure S2D). Similar to chloroquine, siLDHB induced both pro-apoptotic (Figures 2C and 2D) and antiproliferative (Figure 2E) effects on SiHa cells.

To demonstrate that LDHB controls autophagy in cancer cells, we first determined the abundance of LC3-II, a protein recruited to autophagic vesicles and a marker of the autophagic flux (Rubinsztein et al., 2009). Silencing LDHB induced leupeptin-sensitive LC3-II protein accumulation in SiHa cells (Figures 2F and S2E), which represented a potent inhibition of the autophagic flux (1.67–0.70) (Figure 2F), and was associated with accumulation of autophagic substrate optineurin (Korac et al., 2013) (Figure 2G). Similar data were obtained using HeLa cells, where autophagic LC3-II flux decreased (Figure S2F) and optineurin degradation was prevented (Figure S2G) by siLDHB.

Next, we tested the selectivity of LDHB versus LDHA in promoting autophagy in cancer cells. Having verified that siLDHB did not alter LDHA expression in SiHa cells (Figure S2A), we repeated autophagic flux experiments using a siRNA targeting LDHA (Figure S2H). siLDHA did not decrease SiHa cell number (Figure 2H) and did not alter the autophagic flux determined with LC3-II (Figure 2I) and optineurin (Figure 2J). Similarly, siLDHB did not alter LDHA expression in HeLa cells (Figure S1C) and siLDHA had no effect on the autophagic flux of these cells (Figures S2H–S2J). Together, these data demonstrate that LDHB but not LDHA controls the basal autophagic flux of oxidative cancer cells.

The control of basal autophagy by LDHB was selective to cancer cells, as siLDHB did not repress the growth and autophagic flux of nonmalignant BJ, HUVEC, and MCF10A cells to the exception of fetal HFL-1 fibroblasts (Figures S2K and S2L). It was confirmed using a second siRNA and doxycycline-induced shLDHB-1 that did not increase the abundance of optineurin except in fetal HFL-1 fibroblasts (Figures S1E and S2M–S2P). Chloroquine caused optineurin accumulation only in HFL-1 fibroblasts, resulting in cell death (Figures S2N and S2P); it also reduced the number of MCF10A cells but independently of optineurin accumulation (Figures S2M and S2O).

LDHB Controls Autophagic Vesicle Maturation

We examined vesicle trafficking to understand how LDHB regulates autophagy. During autophagy, lysosomes fuse with autophagosomes to form autolysosomes containing active proteases. LDHB was expressed in the lysosomal fraction of SiHa cells (Figure 3A). Silencing of LDHB caused the accumulation of vesicles (Figure 3B) that were acidic (Figure 3C) and expressed the lysosomal marker LAMP-1 (Figure 3D). Acidic vesicle accumulation was also observed with chloroquine, with no additive effects of siLDHB on chloroquine (Figure 3C), suggesting that both treatments induce a lysosomal dysfunction that results in lysosome accumulation. Overexpressing LDHB had the opposite effect; it decreased the number of acidic vesicles per cell (Figures 3C and S3A). Of note, siLDHB did not affect the subcellular distribution pattern of lysosomes (distance to cell nucleus, Figure 3E).

Because there was no additive effect of siLDHB on the genetic disruption of autophagy by siULK1, which targets an early step of autophagy (Figure 2B), and no additive effect of siLDHB on autophagy inhibition by chloroquine, which inhibits lysosomal activity (Figure 2A), we hypothesized that LDHB controls autophagic vesicle maturation. Accordingly, siLDHB repressed the fusion between lysosomes and autophagosomes, which was demonstrated by a decrease in the number of vesicles that coexpressed LAMP-1 and LC3 (Figure 3F). Similarly to chloroquine, siLDHB also decreased the abundance of mature autolysosomes measured using a LC3-mRFP-GFP reporter (Kimura et al., 2007) (Figure 3G). Defective fusion was associated with the accumulation of lysosomes (Figure 3D) and LC3-positive autophagosomes (Figure 3H). siLDHB decreased intracellular proteolysis, which was demonstrated by decreased DQ-BSA dequenching (Figures 3I and S3B), whereas the early endocytic pathway was intact (Figure S3C).

Together, these data show that siLDHB induces lysosomal inhibition in oxidative cancer cells, thus positioning LDHB as an important contributor to lysosomal activity. This conclusion is supported by the fact that LDHB overexpression increased mature autolysosome formation (Figures 3J and S3D) and intracellular proteolysis (Figures 3K and S3E) in SiHa and in HeLa cells.

LDHB Actively Controls Lysosomal Activity in Oxidative Cancer Cells

To test whether LDHB controls the lysosomal function through its enzymatic activity, we first produced vectors encoding HA-tagged catalytically inactive halves of the protein (hLDHBΔ163-331 and hLDHBΔ1-162). While re-expressing full-length LDHB

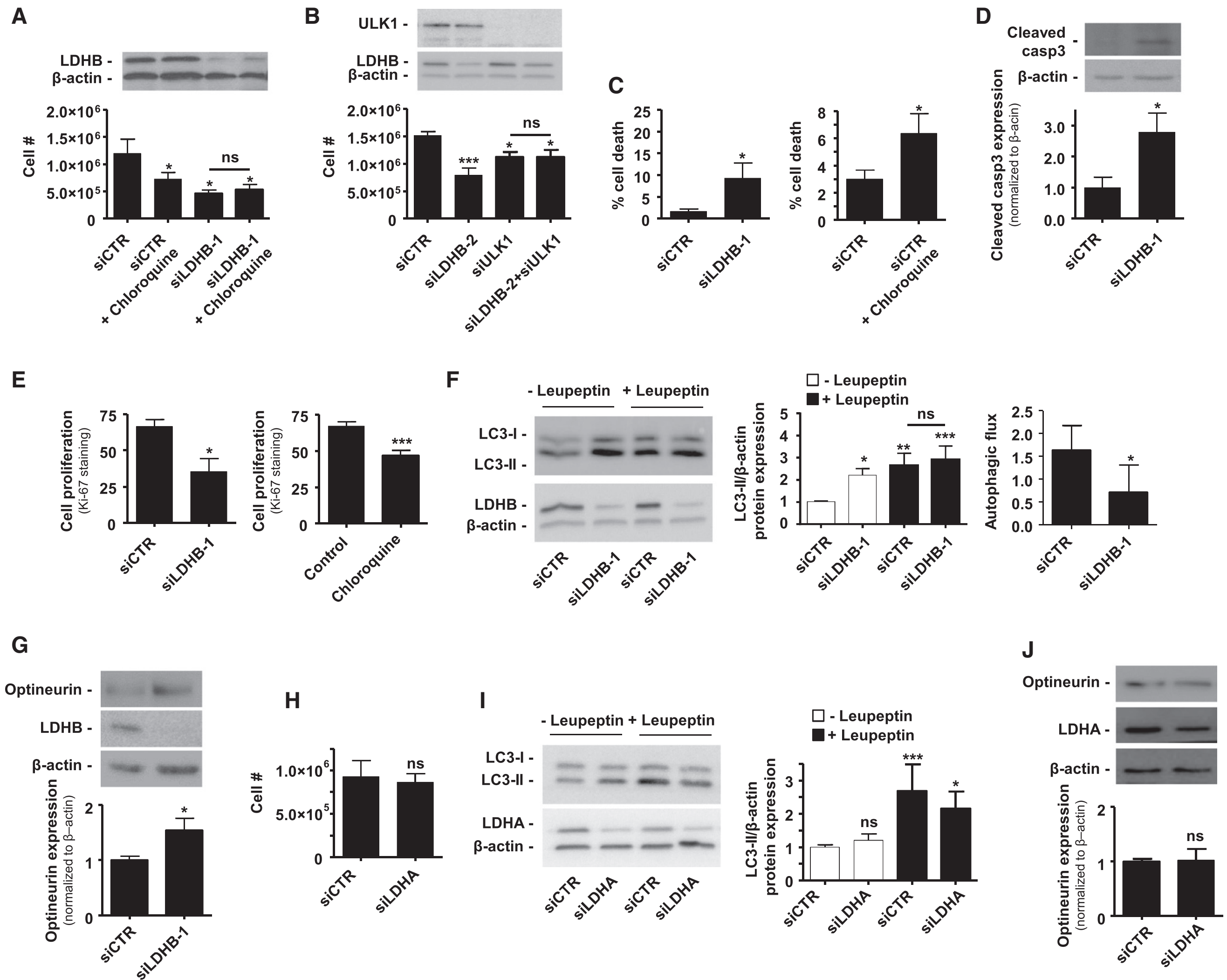

Figure 2. Silencing LDHB Inhibits Autophagy in SiHa Oxidative Cancer Cells

(A) Numbers of cells that were transfected for 72 hr with siCTR or siLDHB-1 and treated with or without 20 μM chloroquine for the last 48 hr (n = 6).

(B) Numbers of cells at 72 hr after transfection with siCTR, siLDHB, siULK1, or siLDHB + siULK1 (n = 5).

(C) Cell death measured by trypan blue exclusion of cells transfected as indicated and then treated with or without 20 μM chloroquine for 48 hr (n = 9–12).

(D) Representative western blot and quantification of cleaved caspase-3 of cells at 72 hr after transfection as indicated (n = 3).

(E) Cell proliferation evaluated by Ki-67 staining in cells with transfection for 72 hr or treatment with or without 20 μM chloroquine for 48 hr as indicated (n = 3).

(F) LDHB, LDHA, LC3-I, and LC3-II protein expression in cells treated overnight with or without leupeptin (150 μM) (n = 13). Autophagic flux was calculated as the difference in LC3-II expression between conditions with and without leupeptin.

(G) Optineurin protein expression in cells transfected with siCTR or siLDHB-1 (n = 8).

(H) Numbers of cells 72 hr after transfection with siCTR or siLDHA (n = 6).

(I) Western blot quantification of LDHA and LC3-II in cells transfected as indicated and treated overnight with or without leupeptin (150 μM) (n = 4).

(J) Optineurin and LDHA protein expression (n = 4).

All data represent means ± SEM. *$p < 0.05$, **$p < 0.01$, ***$p < 0.005$; ns, not significant, by one-way ANOVA and Holm-Sidak's multiple comparisons test (A and B), two-tailed unpaired Student's t test (C–E and H), Kruskal-Wallis and Dunn's multiple comparisons test (F middle, I), or Mann-Whitney test (F right, G, and J). See also Figure S2.

effectively restored the number of SiHa cells transfected with an siRNA targeting the 5′-untranslated sequence of *LDHB* mRNA, neither hLDHBΔ163-331 nor hLDHBΔ1-162 restored cell number (Figures 4A, S4A, and S4B). LDHB overexpression enhanced siCTR cell number. In addition, the MCT1 inhibitor α-cyano-4-hydroxycinnamate (CHC), known to inhibit lactate uptake in SiHa cells (Sonveaux et al., 2008), decreased cell number with no additional effect of siLDHB (Figure 4B). We therefore hypothesized that the enzymatic activity of LDHB promotes lysosome activity.

Upon glucose starvation, a condition stimulating autophagy and increasing lysosomal proteolysis in SiHa cells (Figure S4C), siLDHB decreased SiHa cell number (Figure 4C). Conversely, delivering exogenous lactate activated intracellular proteolysis

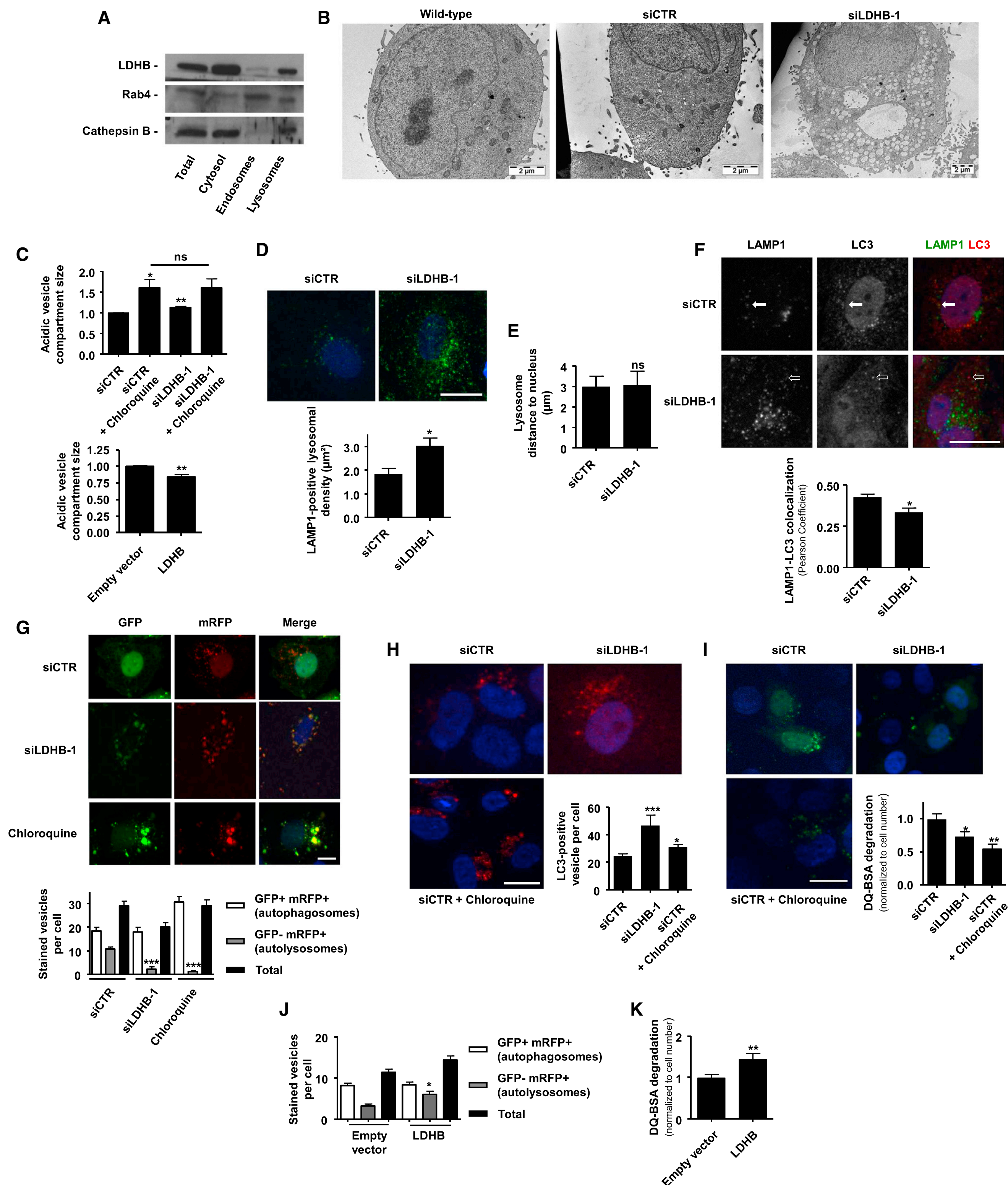

Figure 3. LDHB Controls Autophagic Vesicle Maturation

(A) Representative immunoblots of subcellular fractions of SiHa cells (n = 3). Rab4 and cathepsin B are used as markers enriched in the endosomal and lysosomal fractions, respectively.

(B) Representative electron micrographs of SiHa cells transfected as indicated (scale bar, 2 μm).

(legend continued on next page)

in glucose-starved (Figure 4D) and in glucose-replenished cells (Figure 4E). Lactate activated intracellular proteolysis in a LDHB-dependent manner (Figure 4E), indicating that lactate oxidation to pyruvate supports autophagy in oxidative cancer cells. Accordingly, lactate triggered autolysosome formation (Figure 4F), whereas CHC caused LC3-II protein accumulation with no additive effect on siLDHB (Figure 4G).

To fully understand the molecular determinants responsible for the control of autophagy by LDHB, we aimed to metabolically restore autophagy in LDHB-depleted SiHa cells. LDHB reaction substrate lactate and product pyruvate did not restore intracellular proteolysis (Figures 4E and 4H), but LDHB-depleted cells had switched to a glycolytic metabolism (Figures S4D and S4E), which, similar to MCT1 inhibition (Sonveaux et al., 2008), can oppose lactate and pyruvate uptake. However, neither cell-permeable methyl-lactate nor methyl-pyruvate restored cell number (Figure S4F) or acidic vesicle compartment size (Figure S4G), indicating that pyruvate downstream of LDHB does not promote autophagy. We therefore focused on the conversion of NAD^+ to NADH + H^+ associated with the oxidation of lactate by LDHB. While lactate induced MCT1-dependent lysosome acidification in the presence of LDHB (Figure 4I), siLDHB decreased the NADH/NAD^+ ratio (Figure 4J), which was associated with lysosome alkalinization (Figures 4K, S4H, and S4I) but unchanged cytosolic pH (Figure 4L). Thus, the LDHB reaction promotes lysosomal acidification.

LDHB Promotes V-ATPase-Dependent Lysosomal Acidification

V-ATPase is the major contributor to lysosome acidification, with two protons translocated for each ATP hydrolyzed (Beyenbach and Wieczorek, 2006). Having found by proximity ligation assay that LDHB is in close proximity to V-ATPase (Figure 5A), we used co-immunoprecipitation and identified a physical interaction between LDHB and V-ATPase (Figure 5B). The V-ATPase inhibitor bafilomycin A1 prevented the lysosomal acidification induced by LDHB overexpression (Figures 5C and S5A), indicating that LDHB promotes V-ATPase-dependent lysosomal acidification. Main active proteases in SiHa cells are cysteine cathepsins B (Figure S5B), the acid-dependent cleavage/activation of which was also repressed by siLDHB (Figure 5D). This observation explains why lactate promotes and siLDHB decreases intracellular proteolysis.

Interestingly, silencing LDHB decreased the number of all the human cancer cell lines that we tested (Figure 1G), including WiDr human colon cancer cells, which are aerobically glycolytic (Warburg effect) (Sonveaux et al., 2008). Therefore, using an isogenic series of cancer cells with different previously characterized metabolic activities (Porporato et al., 2014), we finally aimed to test whether LDHB also controls lysosomal activity in glycolytic cancer cells that do not metabolically depend on lactate oxidation for ATP production (Sonveaux et al., 2008). siLDHB decreased the number of mitochondria-deficient SiHa-ρ0 cells (Figures 5E and S5C) and induced acidic vesicle accumulation (Figure 5F). In addition, siLDHA also decreased the number of glycolytic SiHa-ρ0 cells with no additive effect of chloroquine (Figures 5G and S5C), but not the number of wild-type oxidative SiHa cells (Figure 2H). These results indicate that glycolytic cancer cells use lactate-pyruvate cycling to maintain high lysosomal activity, whereas oxidative cancer cells use extracellular lactate delivered by the glycolytic tumor compartment to support autophagy (Figure 5H).

Finally, we confirmed the therapeutic potential of targeting LDHB in cancer by comparing the antitumor efficacy of chloroquine and TET-on shLDHB-1 and shLDHB-3 on established HCT116 tumors in mice, thus using the same model as in Figures S1A and S1B but with two other shRNAs. Chloroquine and/or doxycycline were administered 13 days after tumor implantation once tumors reached 5 mm in diameter. Silencing LDHB with shLDHB-1 or shLDHB-3 was more potent to retard HCT116 tumor growth than chloroquine delivered at a dose of 25 mg/kg every 3 days, and chloroquine did not significantly enhance the effects of shLDHB-1 and shLDHB-3 (Figure 5I). Analysis of tumor biopsies at the end of the treatments confirmed that the two shRNAs inhibited autophagy in vivo, as they reduced the level of ATG12 (Figures 5J and 5K), which is involved in autophagosome formation (Geng and Klionsky, 2008) and is decreased when autophagy is blocked (Ciccia et al., 2014; Aravindan et al., 2015). Conversely, tumors expressing shLDHB significantly accumulated LC3-II (Figure 5L), with an increased number of LC3 foci in cancer cells (Figure 5M), and accumulated optineurin (Figure S5G), indicating a blockage in the degradation process. These differences were not seen when autophagy

(C) Acidic vesicle content measured using acridine orange staining in SiHa cells transfected as indicated and treated with or without 20 μM chloroquine for 48 hr (top graph, n = 4; bottom graph, n = 3).

(D) Representative images of LAMP1 immunostaining and quantification of lysosome density in SiHa cells transfected as indicated (scale bar, 20 μm; n = 3).

(E) Quantification of lysosome distance to nucleus of images obtained in (D) (n = 3).

(F) Evaluation of lysosome-autophagosome fusion in SiHa cells transfected as indicated using LAMP1 and LC3 immunostaining and Pearson correlation coefficient calculation. Closed and open arrows show mature and immature autophagosomes, respectively (scale bar, 20 μm; n = 3).

(G) The abundance of autophagosomes and autolysosomes was measured with an LC3-GFP-mRFP reporter in SiHa cells transfected or treated with or without 20 μM chloroquine for 48 hr as indicated (scale bar, 10 μm; n = 4).

(H) Representative images of LC3 immunostaining and quantification of LC3-positive vesicles in SiHa cells transfected or treated with or without 20 μM chloroquine for 48 hr as indicated (scale bar, 10 μm; n = 3).

(I) Representative images and quantification of intracellular proteolysis by DQ-BSA dequenching in SiHa cells treated with or without 20 μM chloroquine for 48 hr (scale bar, 20 μm; n = 3).

(J) Autophagosomes and autolysosomes abundance measured with an LC3-GFP-mRFP reporter in SiHa cells 48 hr after transfection (n = 4).

(K) Intracellular proteolysis measured with DQ-BSA in SiHa cells 48 hr after transfection (n = 3).

All data represent means ± SEM. $^*p < 0.05$, $^{**}p < 0.01$, $^{***}p < 0.005$; ns, not significant, Kruskal-Wallis with Dunn's test (C, G, I, and J), Mann-Whitney test (C and K), two-tailed unpaired Student's t test (D–F), or one-way ANOVA with Holm-Sidak's multiple comparisons test (H).

See also Figure S3.

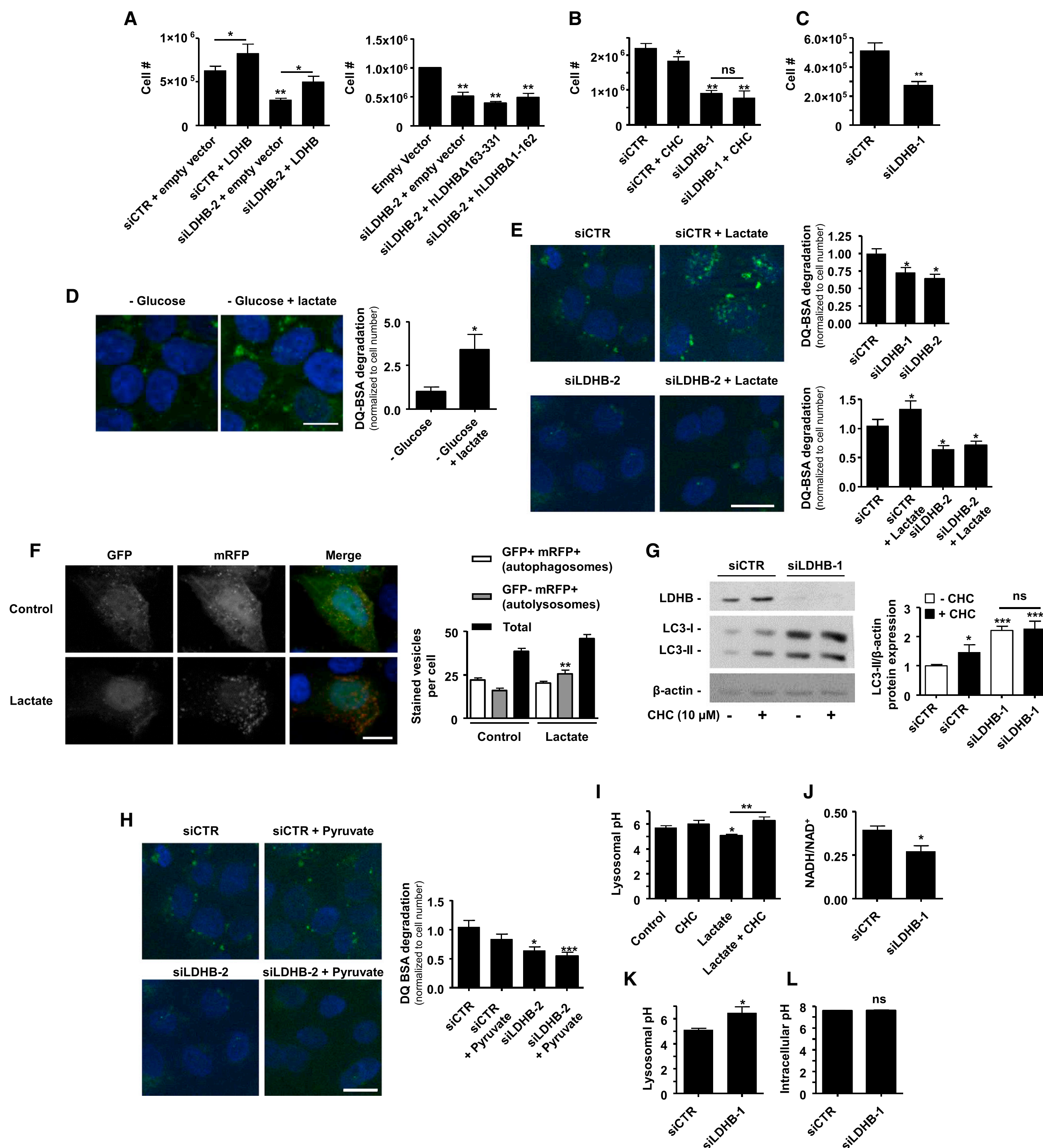

Figure 4. Lactate Promotes LDHB-Dependent Autophagy in Oxidative Cancer Cells

(A) Numbers of SiHa cells transfected with indicated siRNA without or with ectopic expression of LDHB, hLDHBΔ163-331, or hLDHBΔ1-162 (n = 5–7).

(B) Numbers of SiHa cells transfected with indicated siRNA and then treated with or without 10 μM CHC for 48 hr (n = 6).

(C) Numbers of SiHa cells transfected as indicated after glucose and serum starvation for 6 hr (n = 6).

(D and E) Representative images and quantification of intracellular proteolysis by DQ-BSA in SiHa cells grown without (D) or with (E) glucose and with or without treatment with 10 mM lactate (scale bars, 20 μm; 48 hr treatment, n = 4 per group).

(F) Abundance of autophagosomes and of autolysosomes measured with LC3-GFP-mRFP in SiHa cells treated with or without 10 mM lactate for 48 hr (scale bar, 20 μm; n = 4).

(G) LDHB, LC3-I, and LC3-II protein abundance in SiHa cells treated with or without 10 μM CHC for 48 hr (n = 4).

(legend continued on next page)

was inhibited by chloroquine treatment in mice (Figures 5J–5M and S5D–S5G). Together, our results demonstrate that LDHB is a credible target for autophagy inhibition in cancer.

DISCUSSION

Our study positions LDHB as a key contributor to lysosomal activity and autophagy in cancer. Lysosomal acidification depends on LDHB activity both in oxidative cancer cells and in glycolytic cancer cells, and silencing LDHB selectively inhibits the proliferation of cancer compared with normal differentiated cells, thus unraveling LDHB as a promising anticancer target. For therapy, LDHB inhibitors would offer a targeted and more selective alternative to the lysosomotropic agent chloroquine and its derivatives, which act as weak bases. Indeed, chloroquine exerts side effects that are independent of autophagy inhibition (Maycotte et al., 2012; Maes et al., 2014), and its activity decreases with tumor acidity (Pellegrini et al., 2014).

LDHB is a key component of the oxidative pathway of lactate that controls metabolic cooperativeness between glycolytic and oxidative cancer cells (Sonveaux et al., 2008; Leite et al., 2011). In the metabolic cooperation where oxidative cancer cells use lactate preferentially to glucose, getting access to glucose is a clear metabolic advantage for glycolytic cancer cells. In turn, we report that oxidative cancer cells get a high autophagic flux as a metabolic reward. Mutual benefit resulting from lactate exchanges between different types of cancer cells substantiates the hypothesis of a metabolic symbiosis (Sonveaux et al., 2008). According to the extended version of the model (Figure 5H), lactate produced glycolytically diffuses to the oxidative cancer cell compartment, enters into oxidative cancer cells preferentially via MCT1, and lactate and NAD^+ are converted to pyruvate, NADH, and H^+ by LDHB. While pyruvate and NADH fuel oxidative mitochondrial metabolism (Sonveaux et al., 2008; Van Hee et al., 2015), protons promote V-ATPase-dependent lysosomal acidification and autophagy, which is facilitated by a close interaction between LDHB and V-ATPase at the lysosomal surface. In oxygenated cancer cells that rapidly oxidize lactate, a high autophagic flux would primarily facilitate the recycling of damaged cellular components (Rabinowitz and White, 2010). High oxidative activities are indeed associated with elevated oxidative stress, and a major function of autophagy is to recycle oxidized proteins and organelles (Navarro-Yepes et al., 2014).

In oxidative cancer cells, LDHB couples lactate oxidation with autophagy not only when extracellular lactate is provided at a clinically relevant concentration (Walenta and Mueller-Klieser, 2004) (lactate-induced autophagy) but also under basal conditions when low levels of lactate are available (basal autophagy). Comparatively, glycolytic cancer cells generate high amounts of intracellular lactate from pyruvate via the LDHA reaction. Lactate can either be exported, primarily via MCT4 to support metabolic symbiosis, or it can be oxidized back to pyruvate by LDHB (Figure 5H). At first glance, this could be seen as a futile cycle, but it is not. LDHB is indeed needed to sustain autophagy and glycolytic cancer cell survival. In the process, similar to what happens in oxidative cancer cells, lactate and NAD^+ are converted to pyruvate, NADH, and H^+ by LDHB. Protons generated by LDHB promote V-ATPase-dependent lysosomal acidification and autophagy which, in these cells that often reside in metabolically restricted microenvironments, would constitute an additional source of energetic and biosynthetic precursors (Rabinowitz and White, 2010). Transferring protons to lysosomes would also contribute to the pH homeostasis of the cytosol (Spugnini et al., 2014).

Blocking basal autophagy can kill cancer cells (Avalos et al., 2014), and we report that silencing LDHB inhibits basal autophagy and cancer cell proliferation and induces apoptotic cell death. Three characteristics of the response are remarkable. First, silencing LDHB is as effective as chloroquine in inhibiting autophagy. Second, silencing LDHB generally impairs the expansion of human cancer cell lines. Of note, we found that MCF7 cells that are relatively non-dependent on autophagy (Yang et al., 2011; Mancias et al., 2014; Maycotte et al., 2014) are the least sensitive; and autophagy-dependent, Ras-mutated HCT116 cells (Guo et al., 2011) are the most sensitive to LDHB silencing. Third, silencing LDHB shows selectivity for cancer versus normal differentiated cells. Thus, compared with chloroquine and its derivatives that are currently undergoing clinical trials but act in a non-targeted and non-specific manner, targeting LDHB could offer a unique opportunity to inhibit a precise target controlling lysosomal activity and autophagy preferentially in cancer cells. Compared with other components of lactate metabolism, we propose LDHB as a preferred target to simultaneously inhibit autophagy in glycolytic and oxidative cancer cells. In comparison, inhibiting LDHA or MCT4 would decrease the autophagic flux only in glycolytic cancer cells, and targeting MCT1 would block autophagy only in oxidative cancer cells. In support of this, LDHB is an independent prognostic marker of overall survival in uterine cancer patients and promotes the progression of several different types of tumors (De Haas et al., 2008; Yoo et al., 2009; Hussien and Brooks, 2011; Isozaki et al., 2012; McCleland et al., 2012; Beronja et al., 2013; Dennison et al., 2013; Koshiyama et al., 2013; McCleland et al., 2013). Previous studies further indicated that complete hereditary deficiency of LDHB has no symptomatic consequences in humans (Okumura et al., 1999; Sudo et al., 1999), thus supporting the future clinical development of pharmacological inhibitors of LDHB.

Similarly to other inhibitors of autophagy that display most of their therapeutic activity in combination with other anticancer therapies (Chen and Karantza-Wadsworth, 2009; Chen et al., 2010; Amaravadi et al., 2011), silencing LDHB had only limited

(H) Intracellular proteolysis in SiHa cells treated with or without 10 mM pyruvate for 48 hr (scale bar, 20 μm; n = 3).
(I) Lysosomal pH measured with FITC-dextran in SiHa cells treated with or without 10 mM sodium lactate with or without 10 μM CHC for 48 hr (n = 4).
(J) $NADH/NAD^+$ ratio measured enzymatically (n = 3).
(K) Lysosomal pH (n = 4).
(L) Intracellular pH measured with SNARF-1-AM (n = 4).
All data represent means ± SEM. *p < 0.05, **p < 0.01, ***p < 0.005; ns, not significant, by one-way ANOVA with Holm-Sidak's multiple comparisons test (A, B, and I), two-tailed unpaired Student's t test (C and J–L), Mann-Whitney test (D), or Kruskal-Wallis with Dunn's multiple comparisons test (E–H). See also Figure S4.

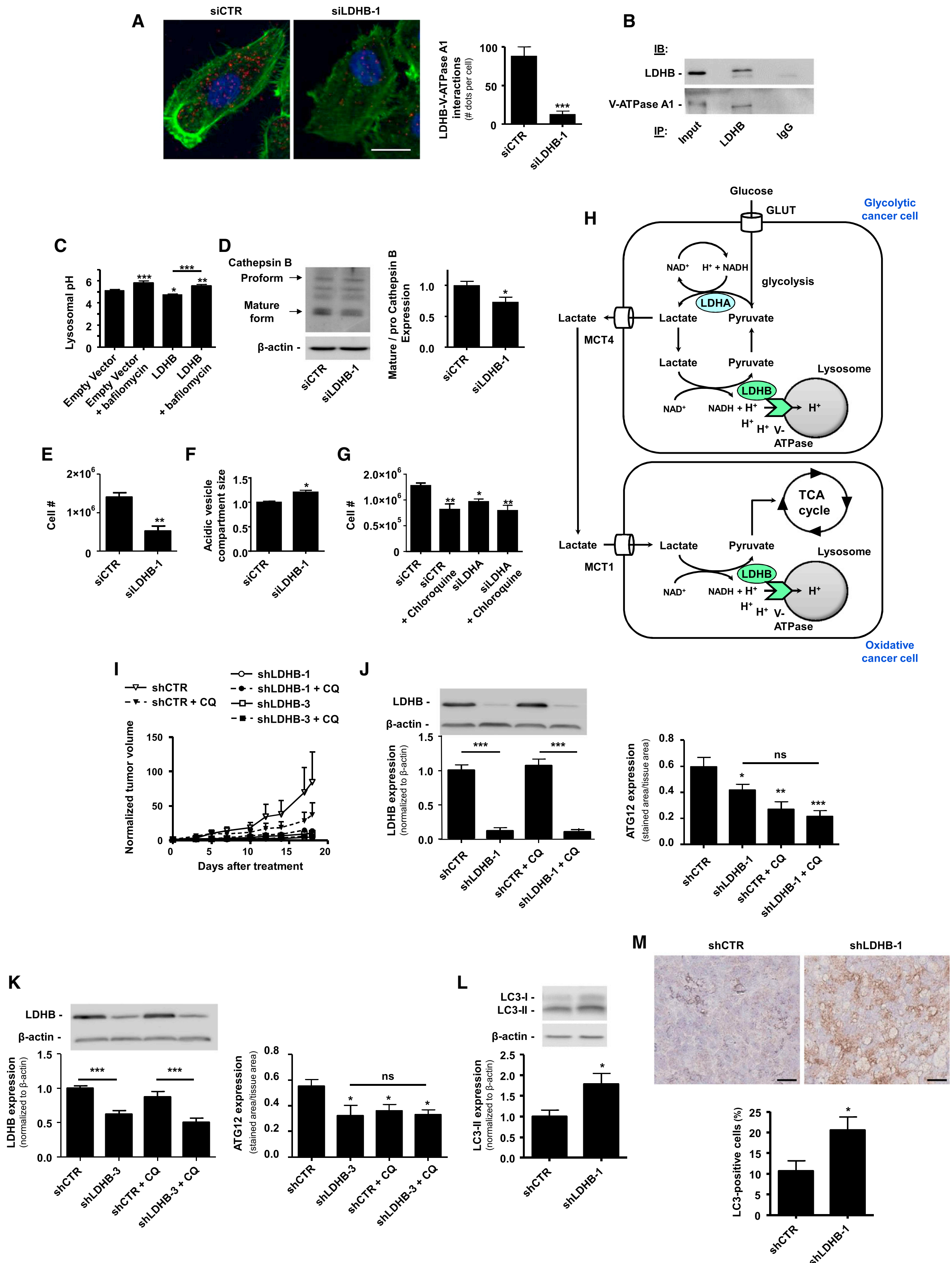

(legend on next page)

effects at the beginning of tumor progression, but stronger effects were seen when silencing was induced at a later time point. Resistance is unlikely to arise from LDHB re-expression or an expressional compensation by LDHA, but could potentially result from metabolic adaptations, in particular switching to a more glycolytic metabolism in an aerobic environment in order to compensate for autophagy inhibition (White, 2012).

Conclusively, we believe that identifying that lactate and LDHB control lysosomal activity and autophagy preferentially in cancer cells lays the ground for promising anticancer applications.

EXPERIMENTAL PROCEDURES

Patient Database Analysis

The SurvExpress gene expression database (Aguirre-Gamboa et al., 2013) was used for the analysis of overall survival in Uterine Corpus Endometrioid Carcinoma TCGA (332 samples). Patients were classified into two risk groups according to gene expression and censored for overall survival without stratification.

In Vivo Experiments

All in vivo experiments were performed with the approval of UCL Comité d'Ethique pour l'Expérimentation Animale (approval ID: TUMETABO) according to national and European animal care regulations. Tumor generation with SiHa and with HCT116 cells expressing shCTR or shLDHB-1 and growth rate determination were conducted as previously described (De Saedeleer et al., 2012). A detailed description of the Experimental Procedures is provided in Supplemental Experimental Procedures.

Cells and Reagents

All cell lines were from ATCC, except SKOV3 human ovarian carcinoma cells (Wintzell et al., 2012), T98G and U373 human glioblastoma cells (Bruyere et al., 2011), and HUVECs (Sigma-Aldrich). Details on culture conditions are provided in Supplemental Experimental Procedures. Unless stated otherwise, all chemicals were from Sigma-Aldrich. To avoid changes in extracellular pH, lactate and pyruvate were used as sodium salts or methylated cell-permeable forms. For functional assays, all data were normalized for cell number or total protein content.

Cell Number, Proliferation, and Apoptosis

Cell number and cell death were measured using trypan blue exclusion on a NucleoCounter device (ChemoMetec). Apoptosis was assayed by measuring caspase-3 cleavage using western blotting. Cell proliferation was evaluated by immunocytochemistry using a mouse monoclonal antibody against Ki-67 (556003, BD Biosciences), and expressed as the percentage of Ki-67-positive cells in the total nuclei count on thresholded images using ImageJ software 1.46r.

RNAi and Cell Transfection

shRNAs were delivered with lentiviruses, and siRNAs and plasmids using transfection. Details are provided in Supplemental Experimental Procedures.

Co-immunoprecipitation and Western Blotting

Co-immunoprecipitation was performed using Dynabeads protein G (Invitrogen) according to the manufacturer's protocol. Immunoblotting was performed as previously described (Feron et al., 1996). Details are provided in Supplemental Experimental Procedures.

Immunochemistry and Proximity Ligation Assay

Immunohistochemistry and immunocytofluorescence labeling were performed as previously described (Sonveaux et al., 2008). In situ protein-protein interactions were detected using the proximity ligation assay (Duolink kit) from Olink Bioscience according to the manufacturer's instructions. Details are provided in Supplemental Experimental Procedures.

Cell Fractionation

Cells fractionation was performed according to Schroter et al. (1999). The procedures are detailed in Supplemental Experimental Procedures.

Electron Microscopy

Transmission electron microscopy was performed using a previously described protocol (Piret et al., 2012).

Endosome, Lysosome, and Autophagic Assays

Endocytic trafficking was measured using a previously described transferrin recycling assay (Magadan et al., 2006). Intracellular proteolysis was quantified based on the intracellular degradation of fluorogenic substrate DQ green BSA (Invitrogen). Acidic vesicles were determined using acridine orange (Sigma) fluorescence measurements, lysosomal pH after overnight endocytosis of 0.5 mg/mL of pH sensitive FITC-dextran (Sigma) by intact cells (Vidal-Donet et al., 2013), and autophagosome maturation with an mRFP-GFP-LC3-encoding construct (Plasmid 21074: ptfLC3; Addgene) used according to Kimura et al. (2007). Cytosolic pH was measured using SNARF-1-AM. Details are provided in Supplemental Experimental Procedures.

Figure 5. LDHB Promotes V-ATPase-Dependent Lysosomal Acidification in Oxidative and Glycolytic Cancer Cells

(A) Representative images of a proximity ligation assay of SiHa cells transfected as indicated. LDHB-V-ATPase A1 protein-protein interactions appear as red dots and F-actin is stained in green with phalloidin-FITC. The graph shows mean number of interactions per cell (scale bar, 20 μm; n = 3).

(B) Co-immunoprecipitation of LDHB with the V-ATPase A1 subunit in SiHa cells (representative of n = 3).

(C) SiHa cells transfected with an empty vector or with a plasmid encoding full-length LDHB. Lysosomal pH was assayed 48 hr later in cells treated overnight with or without 100 nM bafilomycin A1 (n = 4).

(D) Mature and immature lysosomal cysteine cathepsins B detected by immunoblotting in SiHa cells transfected as indicated (n = 5).

(E–G) Cell number (n = 3) (E), cell content in acidic vesicles measured using acridine orange staining (n = 3) (F), and cell number after a treatment with or without 20 μM chloroquine for 48 hr (n = 6) (G) of SiHa-ρ0 cells.

(H) Model describing the contribution of LDHB to lysosomal activity in a metabolic symbiosis based on lactate exchange between glycolytic and oxidative cancer cells.

(I) Mice were implanted with HCT116 cancer cells carrying shCTR, shLDHB-1, or shLDHB-3, and 2 mg/mL doxycycline were administered via the drinking water 13 days after tumor inoculation. Where indicated, 25 mg/kg chloroquine was administered by intraperitoneal injection every 3 days. Each mouse was bearing an shCTR and a shLDHB tumor, and experiments were run simultaneously. The graph depicts tumor growth normalized to tumor size at treatment initiation (n = 6–14 mice per group).

(J and K) Western blot analysis of LDHB expression and immunohistochemical detection of ATG12 expression in shLDHB-1 and matched shCTR (J, n = 8) or shLDHB-3 and matched shCTR (K, n = 6) tumors at the end of the experiment shown in (I).

(L and M) Western blot (L) and immunohistochemistry (M) analysis of LC3-I and LC3-II in the shLDHB-1 and matched shCTR tumors at the end of the experiment shown in (I) (n = 8; scale bar, 20 μm).

All data represent means ± SEM. *p < 0.05, **p < 0.01, ***p < 0.005; ns, not significant, by two-tailed unpaired Student's t test (A, D, E, L, and M), Mann-Whitney test (F), one-way ANOVA with Holm-Sidak's multiple comparisons test (C, G, J, and K).

See also Figure S5.

Metabolic Assays

For metabolic assays, an equal number of cells were plated in 6-well plates in fresh medium. Seventy-two hours later, glucose and lactate concentrations were measured in deproteinized cell supernatants using specific enzymatic assays on a CMA600 Microdialysis Analyzer (CMA Microdialysis). Data were normalized to final cell numbers.

LDHB Activity

LDHB activity was measured in intact cells using the NADH/NAD^+ ratio that was quantified in clear cell lysates using the NAD/NADH Quantitation Kit from Source Bioscience according to manufacturer's instructions. In cell lysates, measurements of LDHB activity were performed using the lactate dehydrogenase B activity assay kit (Abcam) following manufacturer's instructions.

Statistics

All data were normalized to control and presented as means ± SEM; n corresponds to the number of independent experiments. In some figures, the SEM is smaller than the symbols. Two-tailed unpaired Student's t test, Mann-Whitney test, Wilcoxon signed rank test, one-way ANOVA followed by Holm-Sidak's multiple comparison test, Kruskal-Wallis followed by Dunn's multiple comparison test, and two-way ANOVA were used where appropriate. A log rank test was used to compare survival curves. $p < 0.05$ was considered to be statistically significant. Methods and any associated references are available in Supplemental Information.

SUPPLEMENTAL INFORMATION

Supplemental Information includes Supplemental Experimental Procedures and five figures and can be found with this article online at http://dx.doi.org/10.1016/j.ccell.2016.08.005.

AUTHOR CONTRIBUTIONS

T.C. made initial observations that were decisive in conceptualizing the study. L.B. conducted all experiments. L.B., P.B., M.S., P.D., V.V.H., J.F., C.B., P.E.P., T.C., and P.S. designed protocols. L.B., P.B., C.D., P.D., M-J.F., V.V.H., T.V., M.T., J.F., C.B., C.M., and T.C. performed experiments and analyzed data. T.C. produced LDHB plasmid constructs. L.B., T.C., R.F., and P.S. designed constructs derived from LDHB. L.B. and P.S. wrote the manuscript. L.B., P.B., M.S., C.D., P.D., M.-J.F., V.V.H., T.V., M.T., J.F., C.B., P.E.P., R.F., C.M., T.C., and P.S. edited and approved the manuscript. P.S. obtained all grants and supervised the study.

ACKNOWLEDGMENTS

This work was supported by ERC Starting Grant No. 243188 TUMETABO, IAP grant #UP7-03 from the Belgian Science Policy Office (Belspo), an Action de Recherche Concertée from the Communauté Française de Belgique (ARC 14/19–058), the Belgian Fonds National de la Recherche Scientifique (F.R.S.-FNRS, grants 2.5025.12, 3.4567.10, 3.4575.11, 7.4548.13, 7.4507.14), the Belgian Fondation contre le Cancer (2012-186), and the UCL Fonds Spéciaux de la Recherche (FSR). P.S. is a F.R.S.-FNRS Research Associate, and P.E.P, P.B., and P.D. are F.R.S.-FNRS postdoctoral fellows. M.S. and V.V.H. are Télévie Research Fellows. We thank Chantal Fregimilicka and Valéry L Payen for excellent technical assistance, Maria Shoshan (Karolinska Institute, Sweden) for the gift of SKOV3 cells, Florence Lefranc (ULB, Belgium) for T98G and U373 cells, Dominique Lison (UCL) for HFL-1 cells, and the morphology and electron microscopy services of UNamur for electron microscopy analyses.

Received: October 12, 2015
Revised: May 13, 2016
Accepted: August 10, 2016
Published: September 12, 2016

REFERENCES

Aguirre-Gamboa, R., Gomez-Rueda, H., Martinez-Ledesma, E., Martinez-Torteya, A., Chacolla-Huaringa, R., Rodriguez-Barrientos, A., Tamez-Pena, J.G., and Trevino, V. (2013). SurvExpress: an online biomarker validation tool and database for cancer gene expression data using survival analysis. PLoS One *8*, e74250.

Amaravadi, R.K., Lippincott-Schwartz, J., Yin, X.M., Weiss, W.A., Takebe, N., Timmer, W., Dipaola, R.S., Lotze, M.T., and White, E. (2011). Principles and current strategies for targeting autophagy for cancer treatment. Clin. Cancer Res. *17*, 654–666.

Aravindan, S., Ramraj, S.K., Somasundaram, S.T., and Aravindan, N. (2015). Novel adjuvants from seaweed impede autophagy signaling in therapy-resistant residual pancreatic cancer. J. Biomed. Sci. *22*, 28.

Avalos, Y., Canales, J., Bravo-Sagua, R., Criollo, A., Lavandero, S., and Quest, A.F. (2014). Tumor suppression and promotion by autophagy. Biomed. Res. Int. *2014*, 603980.

Beronja, S., Janki, P., Heller, E., Lien, W.H., Keyes, B.E., Oshimori, N., and Fuchs, E. (2013). RNAi screens in mice identify physiological regulators of oncogenic growth. Nature *501*, 185–190.

Beyenbach, K.W., and Wieczorek, H. (2006). The V-type H+ ATPase: molecular structure and function, physiological roles and regulation. J. Exp. Biol. *209*, 577–589.

Bruyere, C., Abeloos, L., Lamoral-Theys, D., Senetta, R., Mathieu, V., Le, M.M., Kast, R.E., Cassoni, P., Vandenbussche, G., Kiss, R., et al. (2011). Temozolomide modifies caveolin-1 expression in experimental malignant gliomas in vitro and in vivo. Transl. Oncol. *4*, 92–100.

Chen, N., and Karantza-Wadsworth, V. (2009). Role and regulation of autophagy in cancer. Biochim. Biophys. Acta *1793*, 1516–1523.

Chen, S., Rehman, S.K., Zhang, W., Wen, A., Yao, L., and Zhang, J. (2010). Autophagy is a therapeutic target in anticancer drug resistance. Biochim. Biophys. Acta *1806*, 220–229.

Ciccia, F., Accardo-Palumbo, A., Rizzo, A., Guggino, G., Raimondo, S., Giardina, A., Cannizzaro, A., Colbert, R.A., Alessandro, R., and Triolo, G. (2014). Evidence that autophagy, but not the unfolded protein response, regulates the expression of IL-23 in the gut of patients with ankylosing spondylitis and subclinical gut inflammation. Ann. Rheum. Dis. *73*, 1566–1574.

Commisso, C., Davidson, S.M., Soydaner-Azeloglu, R.G., Parker, S.J., Kamphorst, J.J., Hackett, S., Grabocka, E., Nofal, M., Drebin, J.A., Thompson, C.B., et al. (2013). Macropinocytosis of protein is an amino acid supply route in Ras-transformed cells. Nature *497*, 633–637.

Curry, J.M., Tuluc, M., Whitaker-Menezes, D., Ames, J.A., Anantharaman, A., Butera, A., Leiby, B., Cognetti, D.M., Sotgia, F., Lisanti, M.P., et al. (2013). Cancer metabolism, stemness and tumor recurrence: MCT1 and MCT4 are functional biomarkers of metabolic symbiosis in head and neck cancer. Cell Cycle *12*, 1371–1384.

De Saedeleer, C.J., Copetti, T., Porporato, P.E., Verrax, J., Feron, O., and Sonveaux, P. (2012). Lactate activates HIF-1 in oxidative but not in Warburg-phenotype human tumor cells. PLoS One *7*, e46571.

De Haas, H.T., Hasselt, N., Troost, D., Caron, H., Popovic, M., Zadravec-Zaletel, L., Grajkowska, W., Perek, M., Osterheld, M.C., Ellison, D., et al. (2008). Molecular risk stratification of medulloblastoma patients based on immunohistochemical analysis of MYC, LDHB, and CCNB1 expression. Clin. Cancer Res. *14*, 4154–4160.

Dennison, J.B., Molina, J.R., Mitra, S., Gonzalez-Angulo, A.M., Balko, J.M., Kuba, M.G., Sanders, M.E., Pinto, J.A., Gomez, H.L., Arteaga, C.L., et al. (2013). Lactate dehydrogenase B: a metabolic marker of response to neoadjuvant chemotherapy in breast cancer. Clin. Cancer Res. *19*, 3703–3713.

Dewhirst, M.W., Cao, Y., and Moeller, B. (2008). Cycling hypoxia and free radicals regulate angiogenesis and radiotherapy response. Nat. Rev. Cancer *8*, 425–437.

Dhup, S., Dadhich, R.K., Porporato, P.E., and Sonveaux, P. (2012). Multiple biological activities of lactic acid in cancer: influences on tumor growth, angiogenesis and metastasis. Curr. Pharm. Des. *18*, 1319–1330.

Feron, O., Belhassen, L., Kobzik, L., Smith, T.W., Kelly, R.A., and Michel, T. (1996). Endothelial nitric oxide synthase targeting to caveolae. Specific interactions with caveolin isoforms in cardiac myocytes and endothelial cells. J. Biol. Chem. *271*, 22810–22814.

Geng, J., and Klionsky, D.J. (2008). The Atg8 and Atg12 ubiquitin-like conjugation systems in macroautophagy. 'Protein modifications: beyond the usual suspects' review series. EMBO Rep. *9*, 859–864.

Guillaumond, F., Leca, J., Olivares, O., Lavaut, M.N., Vidal, N., Berthezene, P., Dusetti, N.J., Loncle, C., Calvo, E., Turrini, O., et al. (2013). Strengthened glycolysis under hypoxia supports tumor symbiosis and hexosamine biosynthesis in pancreatic adenocarcinoma. Proc. Natl. Acad. Sci. USA *110*, 3919–3924.

Guo, J.Y., Chen, H.Y., Mathew, R., Fan, J., Strohecker, A.M., Karsli-Uzunbas, G., Kamphorst, J.J., Chen, G., Lemons, J.M., Karantza, V., et al. (2011). Activated Ras requires autophagy to maintain oxidative metabolism and tumorigenesis. Genes Dev. *25*, 460–470.

Halestrap, A.P., and Wilson, M.C. (2012). The monocarboxylate transporter family–role and regulation. IUBMB Life *64*, 109–119.

Hensley, C.T., Wasti, A.T., and DeBerardinis, R.J. (2013). Glutamine and cancer: cell biology, physiology, and clinical opportunities. J. Clin. Invest. *123*, 3678–3684.

Ho, J., de Moura, M.B., Lin, Y., Vincent, G., Thorne, S., Duncan, L.M., Hui-Min, L., Kirkwood, J.M., Becker, D., Van, H.B., et al. (2012). Importance of glycolysis and oxidative phosphorylation in advanced melanoma. Mol. Cancer *11*, 76.

Hussien, R., and Brooks, G.A. (2011). Mitochondrial and plasma membrane lactate transporter and lactate dehydrogenase isoform expression in breast cancer cell lines. Physiol. Genomics *43*, 255–264.

Icard, P., Kafara, P., Steyaert, J.M., Schwartz, L., and Lincet, H. (2014). The metabolic cooperation between cells in solid cancer tumors. Biochim. Biophys. Acta *1846*, 216–225.

Isozaki, Y., Hoshino, I., Nohata, N., Kinoshita, T., Akutsu, Y., Hanari, N., Mori, M., Yoneyama, Y., Akanuma, N., Takeshita, N., et al. (2012). Identification of novel molecular targets regulated by tumor suppressive miR-375 induced by histone acetylation in esophageal squamous cell carcinoma. Int. J. Oncol. *41*, 985–994.

Kennedy, K.M., Scarbrough, P.M., Ribeiro, A., Richardson, R., Yuan, H., Sonveaux, P., Landon, C.D., Chi, J.T., Pizzo, S., Schroeder, T., et al. (2013). Catabolism of exogenous lactate reveals it as a legitimate metabolic substrate in breast cancer. PLoS One *8*, e75154.

Kimura, S., Noda, T., and Yoshimori, T. (2007). Dissection of the autophagosome maturation process by a novel reporter protein, tandem fluorescent-tagged LC3. Autophagy *3*, 452–460.

Korac, J., Schaeffer, V., Kovacevic, I., Clement, A.M., Jungblut, B., Behl, C., Terzic, J., and Dikic, I. (2013). Ubiquitin-independent function of optineurin in autophagic clearance of protein aggregates. J. Cell Sci. *126*, 580–592.

Koshiyama, A., Ichibangase, T., and Imai, K. (2013). Comprehensive fluorogenic derivatization-liquid chromatography/tandem mass spectrometry proteomic analysis of colorectal cancer cell to identify biomarker candidate. Biomed. Chromatogr. *27*, 440–450.

Krajcovic, M., and Overholtzer, M. (2012). Mechanisms of ploidy increase in human cancers: a new role for cell cannibalism. Cancer Res. *72*, 1596–1601.

Leite, T.C., Coelho, R.G., Da Silva, D., Coelho, W.S., Marinho-Carvalho, M.M., and Sola-Penna, M. (2011). Lactate downregulates the glycolytic enzymes hexokinase and phosphofructokinase in diverse tissues from mice. FEBS Lett. *585*, 92–98.

Levine, B., and Kroemer, G. (2008). Autophagy in the pathogenesis of disease. Cell *132*, 27–42.

Maclean, K.H., Dorsey, F.C., Cleveland, J.L., and Kastan, M.B. (2008). Targeting lysosomal degradation induces p53-dependent cell death and prevents cancer in mouse models of lymphomagenesis. J. Clin. Invest. *118*, 79–88.

Maes, H., Kuchnio, A., Peric, A., Moens, S., Nys, K., De, B.K., Quaegebeur, A., Schoors, S., Georgiadou, M., Wouters, J., et al. (2014). Tumor vessel normalization by chloroquine independent of autophagy. Cancer Cell *26*, 190–206.

Magadan, J.G., Barbieri, M.A., Mesa, R., Stahl, P.D., and Mayorga, L.S. (2006). Rab22a regulates the sorting of transferrin to recycling endosomes. Mol. Cell Biol. *26*, 2595–2614.

Mancias, J.D., Wang, X., Gygi, S.P., Harper, J.W., and Kimmelman, A.C. (2014). Quantitative proteomics identifies NCOA4 as the cargo receptor mediating ferritinophagy. Nature *509*, 105–109.

Maycotte, P., Aryal, S., Cummings, C.T., Thorburn, J., Morgan, M.J., and Thorburn, A. (2012). Chloroquine sensitizes breast cancer cells to chemotherapy independent of autophagy. Autophagy *8*, 200–212.

Maycotte, P., Gearheart, C.M., Barnard, R., Aryal, S., Mulcahy Levy, J.M., Fosmire, S.P., Hansen, R.J., Morgan, M.J., Porter, C.C., Gustafson, D.L., et al. (2014). STAT3-mediated autophagy dependence identifies subtypes of breast cancer where autophagy inhibition can be efficacious. Cancer Res. *74*, 2579–2590.

Mazurek, S. (2011). Pyruvate kinase type M2: a key regulator of the metabolic budget system in tumor cells. Int. J. Biochem. Cell Biol. *43*, 969–980.

McCleland, M.L., Adler, A.S., Shang, Y., Hunsaker, T., Truong, T., Peterson, D., Torres, E., Li, L., Haley, B., Stephan, J.P., et al. (2012). An integrated genomic screen identifies LDHB as an essential gene for triple-negative breast cancer. Cancer Res. *72*, 5812–5823.

McCleland, M.L., Adler, A.S., Deming, L., Cosino, E., Lee, L., Blackwood, E.M., Solon, M., Tao, J., Li, L., Shames, D., et al. (2013). Lactate dehydrogenase B is required for the growth of KRAS-dependent lung adenocarcinomas. Clin. Cancer Res. *19*, 773–784.

Mullen, A.R., Wheaton, W.W., Jin, E.S., Chen, P.H., Sullivan, L.B., Cheng, T., Yang, Y., Linehan, W.M., Chandel, N.S., and DeBerardinis, R.J. (2012). Reductive carboxylation supports growth in tumour cells with defective mitochondria. Nature *481*, 385–388.

Navarro-Yepes, J., Burns, M., Anandhan, A., Khalimonchuk, O., del Razo, L.M., Quintanilla-Vega, B., Pappa, A., Panayiotidis, M.I., and Franco, R. (2014). Oxidative stress, redox signaling, and autophagy: cell death versus survival. Antioxid. Redox Signal. *21*, 66–85.

Okumura, N., Terasawa, F., Ueno, I., Oki, K., Yamauchi, K., Hidaka, H., Tozuka, M., Okura, M., and Katsuyama, T. (1999). Genetic analyses in homozygous and heterozygous variants of lactate dehydrogenase-B (H) subunit–LD-B Matsumoto I and II (LD-B W323R). Clin. Chim. Acta *287*, 163–171.

Pellegrini, P., Strambi, A., Zipoli, C., Hagg-Olofsson, M., Buoncervello, M., Linder, S., and De Milito, A. (2014). Acidic extracellular pH neutralizes the autophagy-inhibiting activity of chloroquine: implications for cancer therapies. Autophagy *10*, 562–571.

Piret, J.P., Vankoningsloo, S., Mejia, J., Noel, F., Boilan, E., Lambinon, F., Zouboulis, C.C., Masereel, B., Lucas, S., Saout, C., et al. (2012). Differential toxicity of copper (II) oxide nanoparticles of similar hydrodynamic diameter on human differentiated intestinal Caco-2 cell monolayers is correlated in part to copper release and shape. Nanotoxicology *6*, 789–803.

Porporato, P.E., Dadhich, R.K., Dhup, S., Copetti, T., and Sonveaux, P. (2011). Anticancer targets in the glycolytic metabolism of tumors: a comprehensive review. Front. Pharmacol. *2*, 49.

Porporato, P.E., Payen, V.L., Perez-Escuredo, J., De Saedeleer, C.J., Danhier, P., Copetti, T., Dhup, S., Tardy, M., Vazeille, T., Bouzin, C., et al. (2014). A mitochondrial switch promotes tumor metastasis. Cell Rep. *8*, 754–766.

Rabinowitz, J.D., and White, E. (2010). Autophagy and metabolism. Science *330*, 1344–1348.

Rubinsztein, D.C., Cuervo, A.M., Ravikumar, B., Sarkar, S., Korolchuk, V., Kaushik, S., and Klionsky, D.J. (2009). In search of an "autophagomometer". Autophagy *5*, 585–589.

Russell, R.C., Tian, Y., Yuan, H., Park, H.W., Chang, Y.Y., Kim, J., Kim, H., Neufeld, T.P., Dillin, A., and Guan, K.L. (2013). ULK1 induces autophagy by phosphorylating Beclin-1 and activating VPS34 lipid kinase. Nat. Cell Biol. *15*, 741–750.

Schroter, C.J., Braun, M., Englert, J., Beck, H., Schmid, H., and Kalbacher, H. (1999). A rapid method to separate endosomes from lysosomal contents using differential centrifugation and hypotonic lysis of lysosomes. J. Immunol. Methods *227*, 161–168.

Sonveaux, P., Vegran, F., Schroeder, T., Wergin, M.C., Verrax, J., Rabbani, Z.N., De Saedeleer, C.J., Kennedy, K.M., Diepart, C., Jordan, B.F., et al. (2008). Targeting lactate-fueled respiration selectively kills hypoxic tumor cells in mice. J. Clin. Invest. *118*, 3930–3942.

Spugnini, E., Sonveaux, P., Stock, C.M., Perez-Sayans, M., De Milito, A., Avnet, S., Garcia, A.G., Harguidey, S., and Fais, S. (2014). Implication of proton channels and exchangers in cancer. Biochim. Biophys. Acta *1848*, 2715–2726.

Sudo, K., Maekawa, M., Houki, N., Okuda, T., Akizuki, S., Magara, T., and Kawano, K. (1999). A novel in-frame deletion mutation in a case of lactate dehydrogenase (LD) H subunit deficiency showing an atypical LD isoenzyme pattern in serum and erythrocytes. Clin. Biochem. *32*, 137–141.

Tan, A.S., Baty, J.W., Dong, L.F., Bezawork-Geleta, A., Endaya, B., Goodwin, J., Bajzikova, M., Kovarova, J., Peterka, M., Yan, B., et al. (2015). Mitochondrial genome acquisition restores respiratory function and tumorigenic potential of cancer cells without mitochondrial DNA. Cell Metab. *21*, 81–94.

Van Hee, V.F., Perez-Escuredo, J., Cacace, A., Copetti, T., and Sonveaux, P. (2015). Lactate does not activate NF-κB in oxidative tumor cells. Front. Pharmacol. *6*, 28.

Vidal-Donet, J.M., Carcel-Trullols, J., Casanova, B., Aguado, C., and Knecht, E. (2013). Alterations in ROS activity and lysosomal pH account for distinct patterns of macroautophagy in LINCL and JNCL fibroblasts. PLoS One *8*, e55526.

Walenta, S., and Mueller-Klieser, W.F. (2004). Lactate: mirror and motor of tumor malignancy. Semin. Radiat. Oncol. *14*, 267–274.

Walenta, S., Snyder, S., Haroon, Z.A., Braun, R.D., Amin, K., Brizel, D., Mueller-Klieser, W., Chance, B., and Dewhirst, M.W. (2001). Tissue gradients of energy metabolites mirror oxygen tension gradients in a rat mammary carcinoma model. Int. J. Radiat. Oncol. Biol. Phys. *51*, 840–848.

Warburg, O. (1956). On the origin of cancer cells. Science *123*, 309–314.

White, E. (2012). Deconvoluting the context-dependent role for autophagy in cancer. Nat. Rev. Cancer *12*, 401–410.

Wintzell, M., Lofstedt, L., Johansson, J., Pedersen, A.B., Fuxe, J., and Shoshan, M. (2012). Repeated cisplatin treatment can lead to a multiresistant tumor cell population with stem cell features and sensitivity to 3-bromopyruvate. Cancer Biol. Ther. *13*, 1454–1462.

Yang, S., Wang, X., Contino, G., Liesa, M., Sahin, E., Ying, H., Bause, A., Li, Y., Stommel, J.M., Dell'antonio, G., et al. (2011). Pancreatic cancers require autophagy for tumor growth. Genes Dev. *25*, 717–729.

Yoo, H.J., Yun, B.R., Kwon, J.H., Ahn, H.S., Seol, M.A., Lee, M.J., Yu, G.R., Yu, H.C., Hong, B., Choi, K., et al. (2009). Genetic and expression alterations in association with the sarcomatous change of cholangiocarcinoma cells. Exp. Mol. Med. *41*, 102–115.

Yoon, Y.H., Cho, K.S., Hwang, J.J., Lee, S.J., Choi, J.A., and Koh, J.Y. (2010). Induction of lysosomal dilatation, arrested autophagy, and cell death by chloroquine in cultured ARPE-19 cells. Invest. Ophthalmol. Vis. Sci. *51*, 6030–6037.